Effect of Deoxidation Sequence on Carbon Manganese Steel Weld Metal Microstructures

Deoxidation sequence has a strong influence on nonmetallic inclusions formation and the subsequent weld refinement

BY F-C. LIAO AND S. LIU

ABSTRACT. During investigation of individual and combined effects of aluminum and titanium on low-carbon low-alloy steel weld metal microstructures, experimental welds were made on 12.7-mm (0.5-in.) thick A516 G70 pressure vessel steel plates using ER70S-3 welding wire and a low-oxygen potential commercial flux. In the aluminum or titanium (individual) addition series welds, the results indicated that the final weld metal microstructures are related to the inclusion size distribution and the amount of aluminum or titanium in solid solution. In the aluminum-titanium or titanium-aluminum (combined) addition welds, deoxidation sequence plays an important role in the formation of specific types of nonmetallic inclusions and in the determination of solid solution elements content, which are fundamental in microstructural refinement.

Introduction

In order to satisfy many critical engineering applications, steel weld metals with high strength and high toughness have been widely investigated in recent years to determine the factors that control weld metal microstructure. During the austenite-to-ferrite decomposition, the first transformation product is grain boundary ferrite (GBF), which forms along prior austenite grain boundaries. Following, Widmanstätten sideplate ferrite (SP) nucleates and grows from grain boundary ferrite as long needle-like laths that protrude into the austenite grains. Grain boundary ferrite and Widmanstätten sideplate ferrite are often grouped together as primary ferrite (PF). As the weld temperature continues to drop, fine acicular ferrite (AF) laths begin to nucleate intragranularly. Finally, the remaining austenite transforms to a variety of microstructural features, which include bainite (B), martensite (M) and pearlite (P). Together with the retained austenite, martensite and carbides form the microconstituents known as MAC. The relative proportions of the different transformation products are strongly influenced by the nonmetallic inclusions in the weld metal.

Several models have been proposed to explain the effects of nonmetallic inclusions such as TiO and $MnO \cdot Al_2O_3$ on the formation of acicular ferrite (Refs. 1–5). However, the influence of deoxidizers (individually or combined) on inclusion formation and inclusion size distribution is still not fully understood. This research focuses on the weld pool deoxidation sequence to better understand the relationship between weld metal microstructures and nonmetallic inclusions.

Weld Pool Deoxidation Practice

In steel making, elements with higher affinity for oxygen than iron are added to the molten metal for the purpose of deoxidation. Some common deoxidizers used in steel making are aluminum, silicon, manganese, and titanium. In arc welding, these same elements are also used for weld pool deoxidation and alloying. They enter the weld pool from the base metal, electrode, or fluxes. In ladle refining of steels, the deoxidation reactions occur at near isothermal and equilibrium conditions quite different from those found in most welding conditions. The nonisothermal, nonequilibrium nature of arc welding makes it very difficult to identify clearly the effect of deoxidation sequence in the weld pool on weld metal microstructure.

In submerged arc welding, oxygen comes mainly from the flux, which may contain easily reduced oxides such as iron oxide, manganese oxide and silica (Ref. 6), which often exist in a dissociated state, that is, metal cations and oxygen anions, in the weld pool. During solidification, the weld pool oxygen concentration established at high temperatures will readjust as a result of decreasing oxygen solubility and the combination of oxygen with deoxidizers that exist in the weld metal. Kluken and Grong (Ref. 7) divided the weld pool into two reaction zones. One is the "hot" reaction zone, immediately beneath the arc, where the deoxidation products are continually separated by highly turbulent flows that sweep those products to the trailing edge of the weld pool. The other is the "cold" reaction zone where most of the precipitated products are entrapped in the weld metal as finely dispersed inclusion particles.

KEY WORDS

Deoxidation Sequence
Weld Metal Microstructure
A516
Chemical Composition
Aluminum Additions
Titanium Additions
Inclusion Composition
Weld Sequence
Transformation
Hardenability

Inclusions Formation

In fusion welding, the level of residual oxygen in liquid iron is strongly dependent on the amount and kind of deoxidizers added. If only one deoxidizer is used in the welding system, the deoxidation sequence

F-C. LIAO and S. LIU are with the Center for Welding and Joining Research, Colorado School of Mines, Golden, Colo.

Paper presented at the 71st Annual AWS Meeting, held April 22–27, 1990, in Anaheim, Calif.

and products are much easier to predict. In reality, however, multiple deoxidizers are used and complex inclusions are formed. The amounts of alloying elements and deoxidizers strongly affect the final inclusion's composition, size, and shape.

Manganese as Deoxidizer

When a steel weld pool is deoxidized by manganese alone, the final deoxidation product will be rich in MnO with a small amount of FeO (Ref. 8). The deoxidation reaction in the weld pool is (Refs. 9,10)

$$Mn_{(l)} + FeO_{(l)} \rightarrow MnO_{(l)} + Fe_{(l)} \quad (1)$$

with

$$\Delta G^{\circ} = -29{,}469 + 13.5T \quad (2)$$

In Equation 2, T is the weld pool temperature. The inclusion type and shape are strongly dependent on the ratio of MnO/FeO. With high manganese level (high $\frac{MnO}{FeO}$), many inclusions will exhibit dendritic morphology (Ref. 11). At a low-manganese level (low $\frac{MnO}{FeO}$), however, the inclusions are always spherical and single phase (Ref. 11).

Silicon as Deoxidizer

If silicon alone is used as the deoxidizer in the welding system, the final deoxidation product in the weld metal is solid silica (Refs. 8,11) and the deoxidation reaction can be written as

$$Si_{(l)} + 2FeO_{(l)} \rightarrow SiO_{2(s)} + 2Fe_{(l)} \quad (3)$$

At the presence of other deoxidizers, however, a liquid silicate product is expected to form.

Aluminum as Deoxidizer

In the case of deoxidation by aluminum, the final products can be Al_2O_3 or a compound of Al_2O_3 and FeO. If the oxygen content is greater than 0.06 wt-%, that is, low aluminum content in the molten metal, $Al_2O_3 \cdot FeO$ is formed, Equation 4 (Ref. 11).

When the residual oxygen content is less than 0.06 wt-%, α-Al_2O_3 is the product, as described in Equation 5 (Ref. 11).

$$2Al_{(l)} + 4FeO_{(l)} \rightarrow Al_2O_3 \cdot FeO_{(s)} + 3Fe_{(l)} \quad (4)$$

$$2Al_{(l)} + 3FeO_{(l)} \rightarrow Al_2O_{3(s)} + 3Fe_{(l)} \quad (5)$$

In low-carbon steel weld pools, where oxygen content is reasonably low, it is common to observe clusters of Al_2O_3 particles.

Titanium as Deoxidizer

Using titanium as the only deoxidizer, a number of oxides are formed. At increasing oxygen content, the following sequence of phases is expected: TiO, Ti_2O_3, Ti_3O_5, TiO_2, $FeO \cdot TiO_2$, and Fe_2TiO_4 (Ref. 11). The final form of the inclusions, however, may be rich in TiO (because of its thermodynamic stability)—Fig. 1.

However, in real arc welding processes, more than one deoxidizer is added to the weld pool and the deoxidation sequence is complicated and most of the inclusions occur in a combined form, with multiple oxides. Some sulfides and oxysulfides may also be present.

Materials and Welding Procedure

The base metal used in this research was an ASTM A516 G70 pressure vessel steel. A 3.2-mm (⅛-in.) diameter ER70S-3 electrode and a high MgO-CaF_2, low SiO_2 commercial flux were used in the experiments. The compositions of the base metal and the welding consumables are given in Table 1.

A two-part experiment concerning the sequence of weld pool deoxidation was designed. The first part examined the titanium-aluminum addition sequence and the second part, the aluminum-titanium addition sequence. In the case of the titanium-aluminum addition sequence welds, the first pass of each weld was made by bead-in-groove submerged arc welding (SAW) to contain eight different levels of titanium, from 0.007 to 0.355 wt-%. The nominal heat input for the first pass welding was approximately 3.0 kJ/mm (76 kJ/in.). The welding parameters are shown in Table 2. After the first passes were made, V-grooves were machined from the center of the beads. Gas tungsten arc (GTA) welds with eight levels of aluminum additions, from 0.009 to 0.228 wt-%, were made with argon shielding with a nominal heat input of approximately 2.9 kJ/mm (74 kJ/in.). GTA welding was chosen to ensure that the variations in oxygen content observed in the second passes were caused mainly by aluminum addition since all other elements were maintained constant. Due to the nonuniform bead shape of some of the second passes, a third autogenous GTA weld pass at 2.9 kJ/mm was applied in the transverse direction of all welds to homogenize the weld metal. The welding sequence is shown schematically in Fig. 2.

The second part of the experiment followed similar procedures as the first part with the exception of the sequence of deoxidizers addition (aluminum in the first pass and titanium in the second pass).

Analyses of the Experimental Welds

For reasons indicated previously, only the first and third passes were studied. They were examined using a light microscope to evaluate quantitatively the volume fractions of the various microstructures. Systematic two-dimensional point counting was performed on each of the weld specimens. Among all quantitative methods available in phase proportions determination, the technique of systematic two-dimensional point counting results in the smallest relative error, approximately ten percent.

The chemical composition of the weld passes were analyzed using an optical emission spectrometer and reported in Table 3. The carbon, sulfur, oxygen, and nitrogen content of the weld metals were determined using interstitial analyzers. Inclusions from the different passes were

Table 1—Chemical Compositions of the Base Plate, the ER70S-3 Electrode, and the Commercial Flux Used in this Research

	C (wt-%)	S (wt-%)	Mn (wt-%)	P (wt-%)	Si (wt-%)	Cr (wt-%)	Mo (wt-%)	Ti (wt-%)	Cu (wt-%)	Al (wt-%)
Base metal A516 G70 PVQ ½ in.	0.257	0.012	1.20	0.008	0.174	0.023	0.002	0.001	0.019	0.028
ER70S-3 Electrode	0.124	—	1.152	0.021	0.56	—	—	—	0.070	0.010
	SiO_2 (wt-%)	Al_2O_3 (wt-%)	MgO (wt-%)	CaO (wt-%)	MnO (wt-%)	TiO_2 (wt-%)	CaF_2 (wt-%)	Na_2O (wt-%)	Fe_2O_3 (wt-%)	C (wt-%)
Commercial flux	10.7	17.3	31.7	6.6	1.1	0.86	24.1	0.78	1.9	0.35

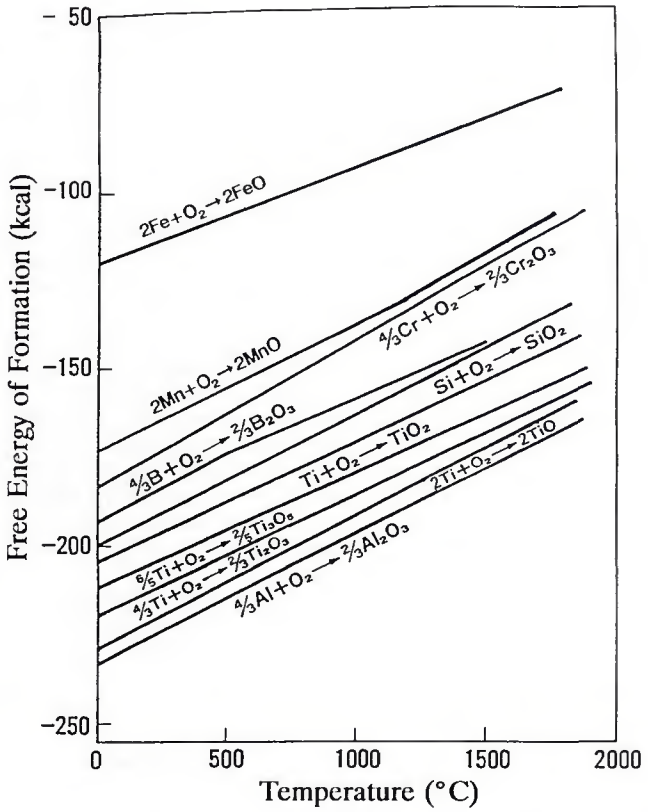

Fig. 1—Free energy of formation of some oxides (Ref. 17).

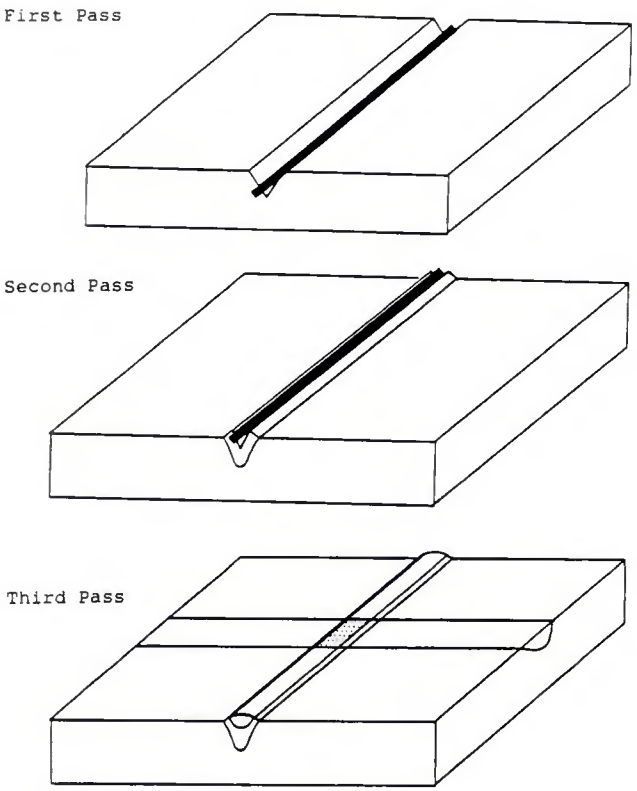

Fig. 2—Schematic drawing of the welding sequence.

Table 2—Summary of Welding Parameters for the Experimental Welds

	Welding Process	Welding Voltage (V)	Welding Current (A)	Travel Speed (mm/s)	Nominal Heat Input (KJ/mm)
First pass	SAW	31	340	3.5	3.0
Second pass	GTAW	16	250	1.4	2.9
Third pass	GTAW	16	250	1.4	2.9

Table 3—Chemical Composition of the Experimental Welds Discussed

Weld	C (wt-%)	Mn (wt-%)	Si (wt-%)	Ti (wt-%)	Al (wt-%)	O (wt-%)	N (wt-%)
t1	0.143	0.84	0.19	0.007	0.005	218	50
t2	0.151	0.88	0.20	0.014	0.007	221	49
t3	0.149	0.95	0.22	0.036	0.009	283	49
T1	0.127	0.90	0.20	0.046	0.006	217	58
T2	0.141	0.85	0.28	0.201	0.012	274	56
a1	0.132	0.88	0.18	0.002	0.009	258	54
a2	0.132	0.88	0.22	0.003	0.013	246	54
a3	0.107	0.88	0.20	0.003	0.026	302	52
A1	0.156	0.96	0.21	0.003	0.039	365	55
A2	0.138	0.87	0.25	0.003	0.054	418	59
a1t1	0.139	0.72	0.14	0.010	0.004	191	68
a1t2	0.118	0.72	0.14	0.043	0.004	179	87
a1t3	0.119	0.67	0.12	0.083	0.004	146	66
t3a1	0.109	0.58	0.12	0.013	0.005	93	52
t3a2	0.148	0.74	0.17	0.022	0.024	188	55
t3a3	0.122	0.64	0.15	0.019	0.033	178	53

isolated using carbon extraction replica technique and analyzed with a scanning electron microscope. A minimum of 500 particles were examined from each weld and the diameter of the particles measured directly on the microscope. The chemical compositions of these inclusions were determined using SEM/EDS (energy dispersive spectroscopy).

Results and Discussion

Individual Effects

Relationship between Weld Metal Chemical Composition and Microstructures

To correlate weld metal microstructures with chemical composition, the hardenability of the weld metals according to the IIW carbon equivalent (CE) equation (Ref. 12) was first considered. Only the welds with similar CE values (0.30 wt-%) were evaluated to determine the aluminum and titanium effects and the results shown in this paper.

In the first pass weldments, Figure 3 shows that there is a threshold concentration of titanium (approximately 0.05 wt-%) above which bainite increased at the expense of acicular ferrite and grain boundary ferrite. The increase in bainite at higher titanium concentrations seems to suggest that titanium in excess of 0.05 wt-% may exist in the form of solid solu-

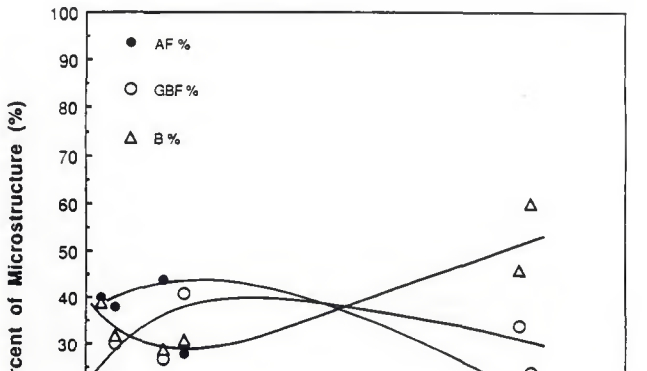

Fig. 3—Variation in weld metal microstructure as a function of weld metal titanium concentration.

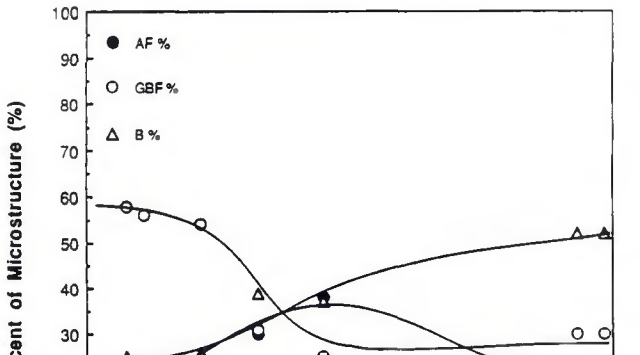

Fig. 4—Variation in weld metal microstructure as a function of weld metal aluminum concentration.

tion and promote the formation of bainite. At low-titanium concentrations, both acicular ferrite and grain boundary ferrite increased at the expense of bainite with titanium addition.

The variation of weld metal microstructures with only aluminum addition is shown in Fig. 4. Below approximately 0.055 wt-% of aluminum, the volume fraction of acicular ferrite and bainite increased with aluminum, while grain boundary ferrite decreased. Above this point, grain boundary ferrite and bainite increased at the expense of acicular ferrite. This result agrees with the data reported by Brownlee (Ref. 13). Figures 5 and 6 are light micrographs taken from specimens with different levels of titanium and aluminum addition. Note that the large amount of fine intragranular features shown in Fig. 5C is not acicular ferrite. More careful examination showed that those are, in fact, bainite, as indicated by the arrows in Fig. 7.

Relationship between Prior Austenite Grain Size and Chemical Composition

Another factor to be considered in weld metal phase transformation is the prior austenite grain size. For a similar heat input (and thus, cooling rate), the different alloying elements and their levels of additions showed different effects on prior austenite grain size. Figures 8 and 9 show the variation of prior austenite grain size as a function of titanium and aluminum addition. In Fig. 8, prior austenite grain size can be observed to decrease with increasing titanium content. Figure 9, however, shows that prior austenite grain size remained approximately constant with aluminum additions. This seems to indicate that the welds with titanium additions may also have inclusion populations that pin the austenite grain boundaries more effectively and restrict austenite growth. The aluminum bearing welds did not exhibit the same behavior. In the case of weld specimens with titanium addition, the austenite grain size observation also agreed with the weld metal microstructure. Large austenite grain size also exhibited smaller amount of grain boundary ferrite. The effect of inclusions on weld metal phase transformations will be discussed in the following paragraphs.

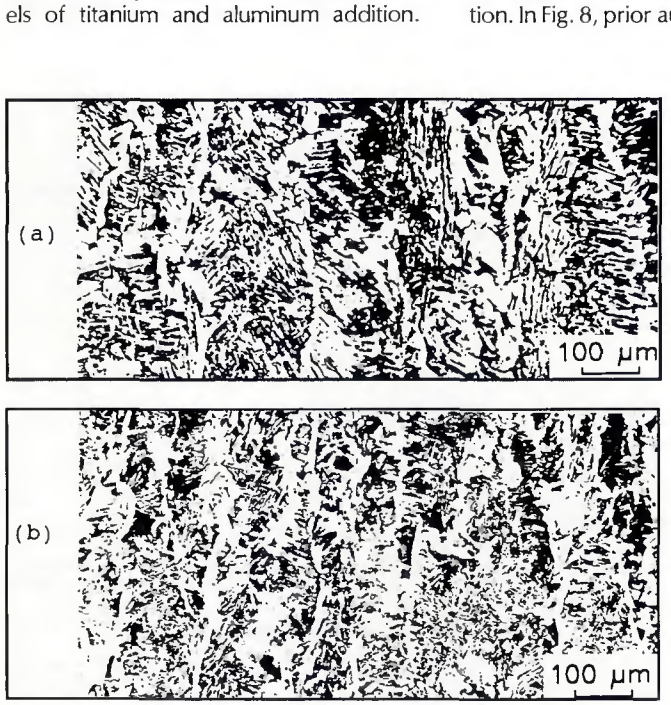

Fig. 5—Weld metal microstructure showing mixture of grain boundary ferrite, PF, SP, acicular ferrite, and bainite for different levels of titanium addition. A—0.007 wt-% (40% AF, 21% PF, 34% B); B—0.014 wt-% (44% AF, 27% PF, 29% B); C—0.201 wt-% (20% AF, 34% PF, 46% B).

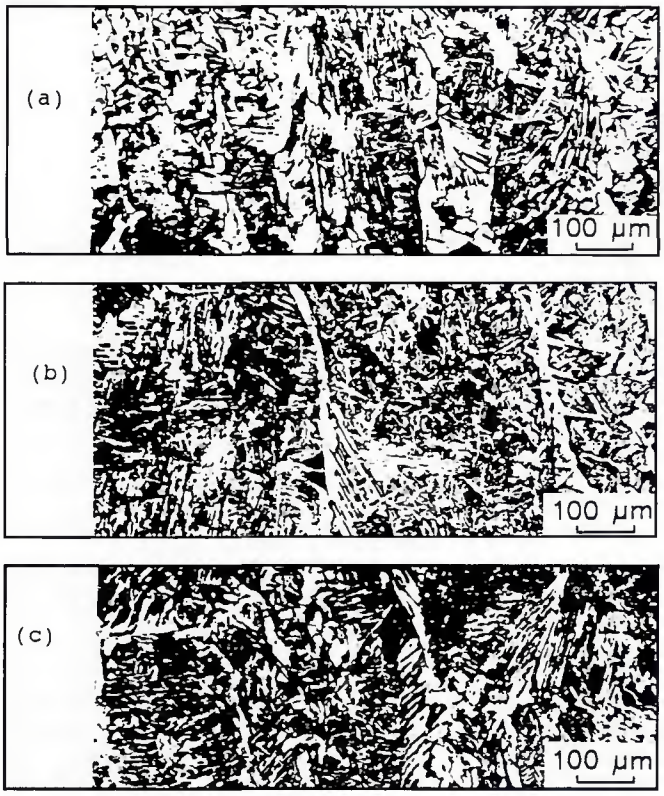

Fig. 6—Weld metal microstructure showing mixture of grain boundary ferrite, PF, SP, acicular ferrite, and bainite for different levels of aluminum addition. A—0.009 wt-%; B—0.054 wt-%; C—0.118 wt-%.

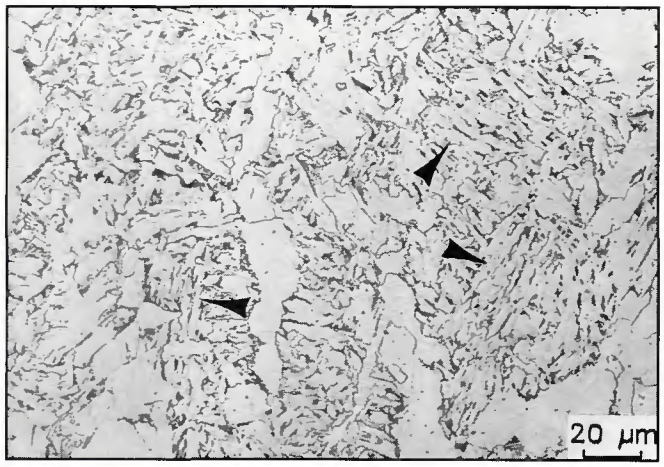

Fig. 7—High magnification micrograph showing that the fine intragranular features shown in Fig. 5C are not acicular ferrite, but rather, bainitic in nature (with carbide between parallel ferrite laths).

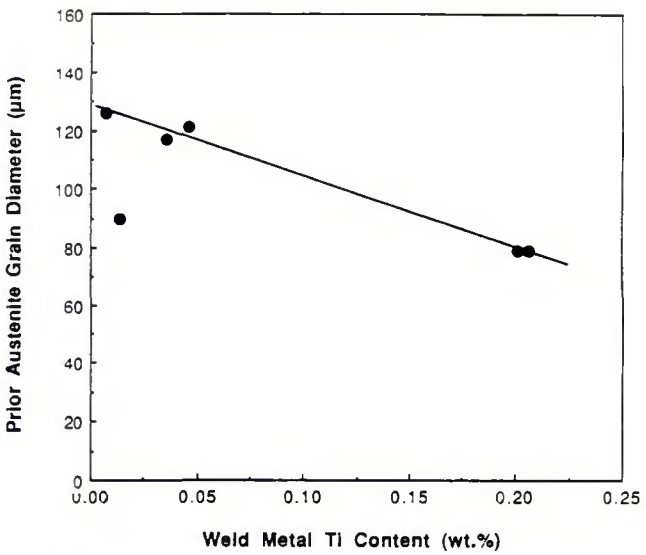

Fig. 8—Variation of prior austenite grain size as a function of weld metal titanium addition.

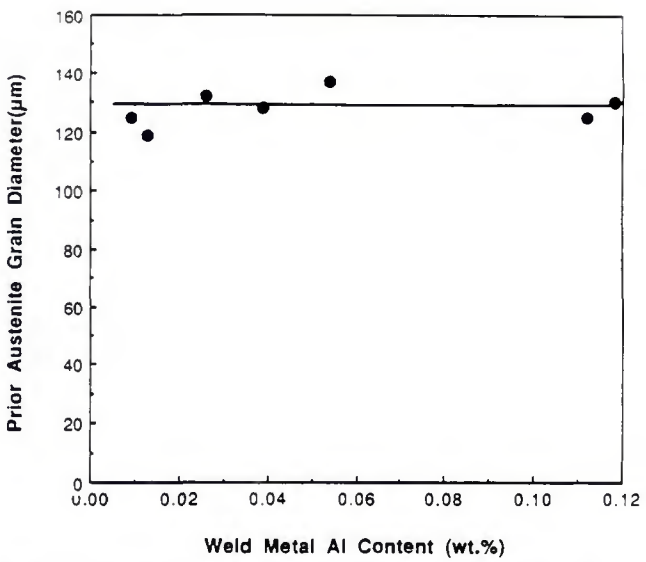

Fig. 9—Variation of prior austenite grain size as a function of weld metal aluminum addition.

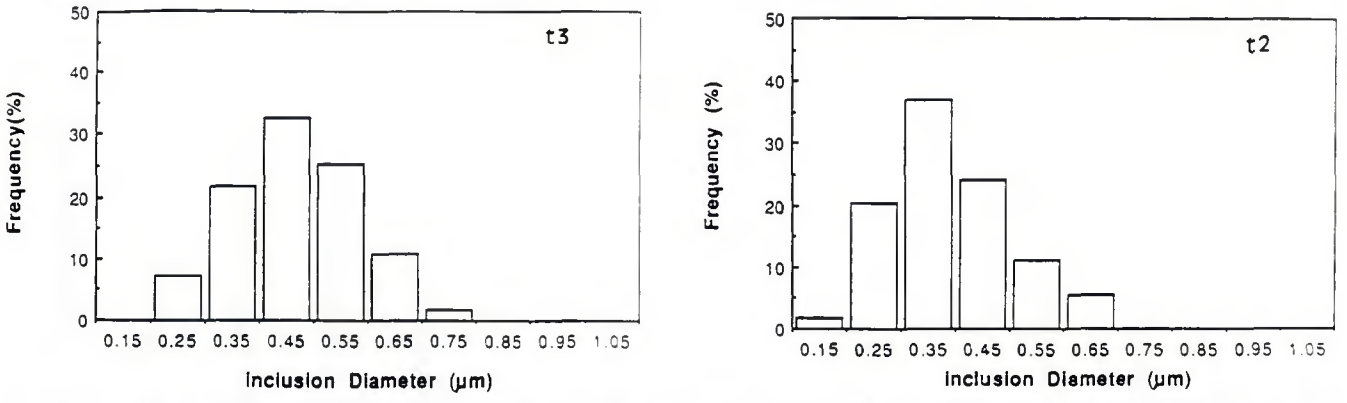

Fig. 10—Simple size distribution of the inclusions extracted from: A—Specimen t3 (Ti = 0.036 wt-%; Al = 0.009 wt-%; B—Specimen t2 Ti = 0.014 wt-%; Al = 0.007 wt-%) with only titanium addition.

Influence of Inclusion Size Distribution on Weld Metal Transformation

From Figs. 10 and 11, it is clear that the aluminum addition series welds exhibited inclusion populations with larger particles than the titanium addition welds (for example, the number of inclusions with diameter larger than 0.7 μm). This observation explains in part the small variation of austenite grain size with weld metal aluminum content, since large inclusions are ineffective in pinning grain boundaries. Figures 10A and 11A show the inclusion size distribution in the optimal titanium and aluminum addition welds, 0.050 and 0.055 wt-%, respectively. No small particles (with diameter <0.2 μm) were observed and the particle size mode of both welds was 0.45 μm. These welds also exhibited higher volume fraction of acicular ferrite than the other welds, which seems to agree with the findings of Barbaro, *et al.* (Ref. 14), and Jang, *et al.* (Ref. 15), that inclusions of diameters within the range of 0.4 to 0.6 μm are more efficient in acicular ferrite formation. Cochrane, *et al.* (Ref. 16), also reported similar particle size range being effective in acicular ferrite nucleation.

At higher aluminum additions, the weld metals exhibited even larger particles, as shown in Fig. 11B, which further supports the discussion that along with inclusion size, the size distribution of the inclusions is also important in defining the final weld metal microstructures.

Influence of Weld Metal Composition on the Inclusion Oxide Types

With the addition of different levels of titanium or aluminum, the chemical constitution of the inclusions was also quite different. In C-Mn-Si steels weld metals, the inclusions contain mainly SiO_2 and MnO. As aluminum is added, the composition of the inclusions were observed to change, with increasing Al_2O_3 content. Cochrane, *et al.* (Ref. 16), observed similar behavior in his investigation. Increasing weld metal titanium concentration led to an enrichment of titanium in the inclusions. TiO is assumed to be the predominant phase in the inclusions because of the many reports in the literature (Refs. 17–19) and the greater thermodynamic stability (ΔG_f) of TiO compared to the other titanium oxides—Fig. 1. Liu and Olson (Refs. 20–21), and Bhatti, *et al.* (Ref. 22), have also observed similar results in their investigations.

Figures 12 and 13 show the variation of oxide types in inclusions as a function of weld metal aluminum and titanium content. To simplify the discussion, it was assumed that only simple oxides such as Al_2O_3, TiO, SiO_2, and MnO resulted during deoxidation and that these oxides combine to form the final inclusions. Figure 12 shows that the amount of Al_2O_3 in the inclusions increased with aluminum addition, while other oxides such as SiO_2, MnO, and TiO decreased. Figure 13 shows that with titanium additions TiO is the main component. Small amounts of Al_2O_3, MnO, and SiO_2 were present but decreased with increasing titanium content.

Combined Effects

Due to the large number of welds made in both the aluminum-titanium (A-T) sequence and titanium-aluminum (T-A) sequence, a typical set was chosen from each group to illustrate the effect of deoxidation sequence on weld metal transformation behavior.

Weld Metal Composition Effect in Aluminum-Titanium Sequence Welds

The A-T sequence welds (a1t1, a1t2, and a1t3) showed that titanium additions

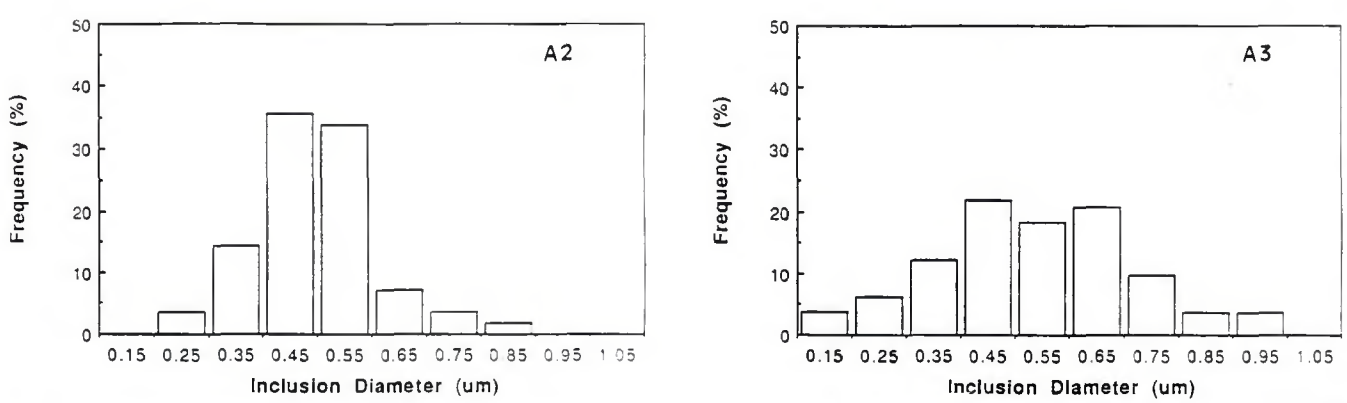

Fig. 11—Inclusion size distribution as a function of weld metal aluminum content. A—Al = 540 ppm and Ti = 30 ppm; B—Al = 1180 ppm and Ti = 30 ppm.

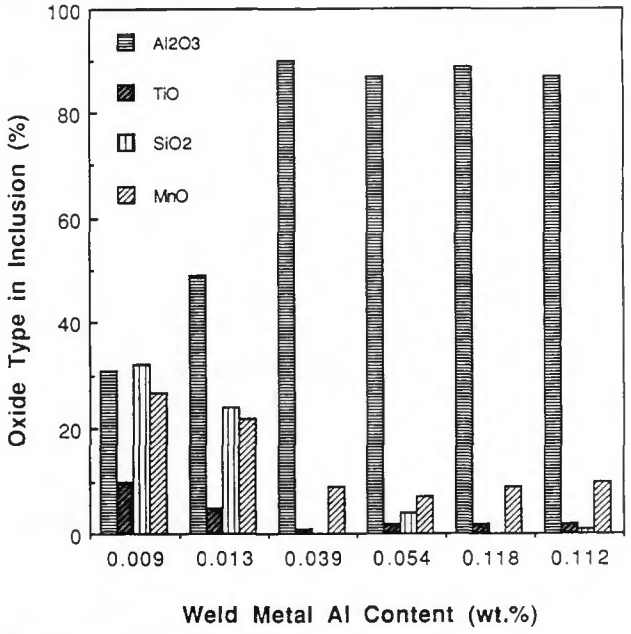

Fig. 12—Effect of weld metal aluminum content on inclusion composition.

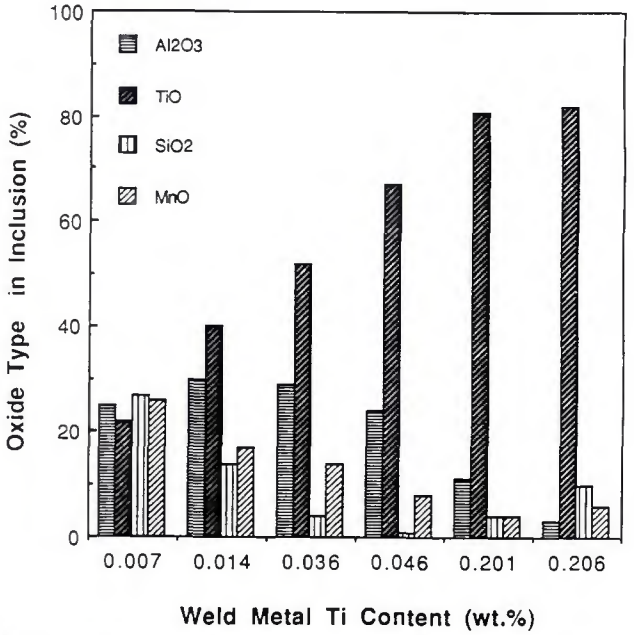

Fig. 13—Effect of weld metal titanium content on inclusion composition.

in the second pass decreased the oxygen content residual from Weld a1. Note that Weld a1 was deoxidized with aluminum alone. With the addition of titanium in the second pass, the oxygen content of Weld a1 was reduced to 191, 179, and 146 ppm in Welds a1t1, a1t2, and a1t3, respectively (indicated as closed circles in Fig. 14). To explain the microstructural changes observed in these welds as a function of oxygen and titanium content, it is assumed that with sufficient oxygen in the system, all aluminum in the weld metal will form the stable Al_2O_3 and that these alumina particles will not be reduced by subsequent titanium addition during the second pass. On the other hand, MnO and SiO_2 formed initially are assumed to be reducible to manganese and silicon by titanium addition. Finally, it is assumed that all titanium atoms in the weld metal are in the form of TiO—Fig. 1.

Chemical analysis showed that the first pass (weld a1 with only aluminum addition) has the following composition: Al = 90 ppm, Ti = 20 ppm, O = 258 ppm, and N = 54 ppm. Of the 258 ppm of oxygen, approximately 80 ppm of oxygen combined with the 90 ppm of aluminum and 7 ppm of oxygen combined with the 20 ppm of titanium. Only 171 ppm of oxygen remained to combine with other elements such as manganese and silicon resulting in MnO and SiO_2. Indeed, the presence of manganese oxide and silica was confirmed by inclusion analyses shown in Fig. 12.

During the second pass welding (a1t1), the oxygen content dropped from 258 to 191 ppm—Fig. 14. The loss could be attributed to the coalescence of inclusions, which were later eliminated by flotation or convective flow in the weld pool. This is verified by the reduction of aluminum from 90 ppm to 40 ppm after

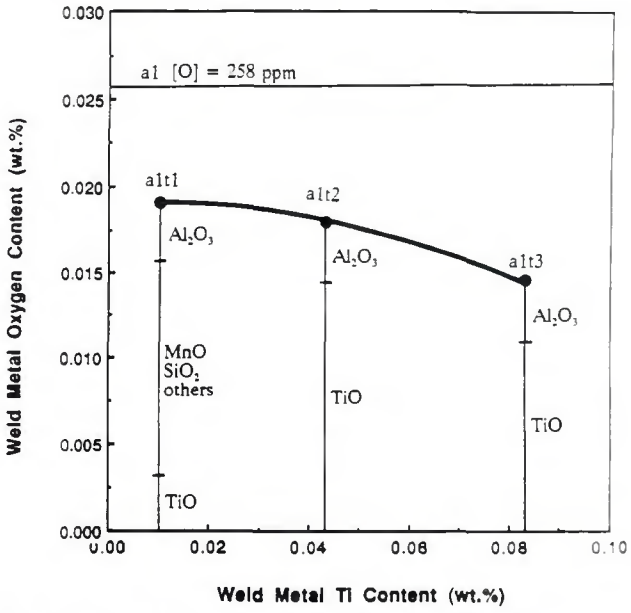

Fig. 14—Variation of weld metal oxygen content as a function of titanium additions in the aluminum-titanium group welds.

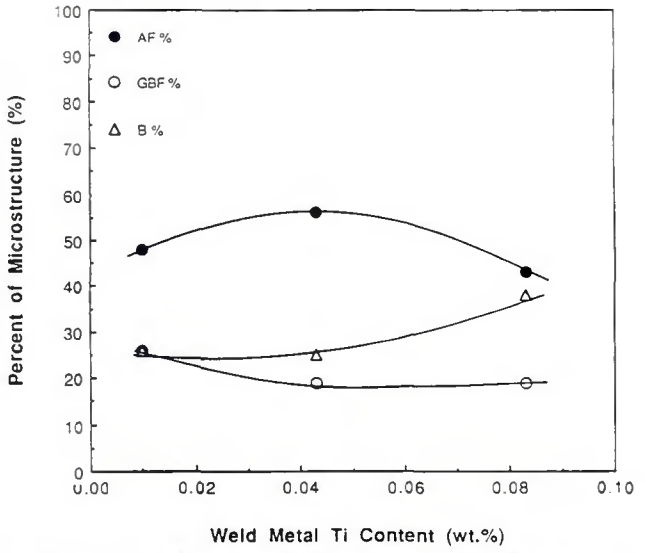

Fig. 15—Variation of weld metal microstructure as a function of titanium additions in the aluminum-titanium group welds.

the titanium addition. In this weld, 36 ppm of oxygen were consumed to form Al_2O_3 with the 40 ppm of aluminum. To react with the 100 ppm of titanium, 33 ppm of oxygen were needed. The remaining oxygen in the second pass combined with manganese and silicon to form MnO and SiO_2, which explains the inclusion analysis reported earlier. The three vertical lines in Fig. 14 were drawn to illustrate the relative amounts of Al_2O_3, TiO, MnO, and SiO_2 that would result in each weld after the addition of the second deoxidizer. The relative proportions of these oxides in the inclusions were also confirmed experimentally in this work.

Increasing titanium addition in the second weld, the amount of residual oxygen decreased further. Weld a1t2 contained 40 ppm of aluminum, 430 ppm of titanium, and 179 ppm of oxygen. Following the procedure described in the previous paragraph, it was determined that 143 ppm of oxygen was necessary to combine with 430 ppm of titanium and no oxygen would be available for other elements. This confirms the observation of numerous titanium-bearing particles in the inclusion population. The increase in acicular ferrite in the weld is then attributed to the larger amount of TiO inclusions in the weld. Since a small amount of MnO and SiO_2 was detected in the inclusions, some titanium must have remained in the weld metal in the form of nitride or solid solution.

Further increasing the titanium content to 830 ppm, Weld a1t3 contained 40 ppm of aluminum and 146 of oxygen. In this weld, 36 ppm of oxygen combined with 40 ppm of aluminum to form Al_2O_3. Assuming that all remaining oxygen atoms reacted with titanium to form TiO, then the 110 ppm of oxygen would have consumed only 330 ppm of titanium. This calculation shows that at least 500 ppm of titanium must have remained in the weld metal, in the form of carbide, nitride, and solid solution.

During solidification, only a fraction of the titanium atoms will form nitride or carbide (as individual particles or on the surface of already existing inclusions) in the liquid steel. Taking into account the solubility product of TiN and TiC in austenite (Ref. 23) and that the nucleation and growth of TiN and TiC are controlled by titanium diffusion (Ref. 24), only part of the titanium atoms will form TiN and TiC on the outer layer of existing inclusions (oxide particles) (Refs. 7,24). The remaining titanium atoms will be dispersed in the weld metal as solid solution atoms and hardenability agent. Experimental evidences of Kluken and Grong (Ref. 7) and Es-Souni and Beaven (Ref. 24) seem to support the above statement. These authors investigated the differences between total and acid soluble contents of aluminum and titanium, and determined

Table 4—Chemical Composition of Selected Experimental Welds Showing the Total and Acid-Soluble Contents of Aluminum and Titanium in Low-Carbon Low-Alloy Steel Weld Metal

C (wt-%)	O (wt-%)	N (wt-%)	Al total (wt-%)	Al soluble (wt-%)	Ti total (wt-%)	Ti soluble (wt-%)
0.09	0.037	0.005	0.02	0.002	0.025	0.018
0.09	0.039	0.005	0.037	0.004	0.022	0.018
0.09	0.040	0.006	0.044	0.006	0.058	0.046
0.10	0.031	0.005	0.062	0.013	0.032	0.029
0.09	0.031	0.006	0.053	0.008	0.053	0.052

that despite the high affinity of titanium for carbon and nitrogen, a significant amount of titanium atoms remain in solution, determined as acid soluble titanium—Table 4 (Ref. 7).

From the calculations above, it is easy to explain the variation of microstructures in Fig. 15. Figure 15 shows that maximum acicular ferrite was observed at approximately 0.042 wt-% of titanium. Above this point, acicular ferrite was replaced by bainite. Below this point, acicular ferrite increased at the expense of grain boundary ferrite. From Fig. 14, TiO was observed to increase with titanium additions at the composition range below 0.04 wt-%, which led to the conclusion that the volume fraction of acicular ferrite increased with increasing TiO. Above the optimal value, uncombined titanium atoms remain in the weld pool and behave as hardenability agent, promoting bainite formation. In all A-T group welds, high-titanium addition led to high-volume fractions of bainite, sometimes close to 100% (Ref. 25).

Weld Metal Composition Effect in Titanium-Aluminum Sequence Welds

The T-A welds (t3a1, t3a2, and t3a3) showed that aluminum increased the second pass weld metal oxygen content to a maximum point followed by a slight drop, as shown in Fig. 16. From Fig. 17, it can be seen that above 0.024 wt-% of aluminum addition, acicular ferrite is replaced by bainite.

Below 0.024 wt-% of aluminum, acicular ferrite increased at the expense of bainite. Grain boundary ferrite did not seem to be affected by aluminum addition.

In the case of Weld t3 (with titanium addition in the first pass), the "residual" composition is Al = 90 ppm, Ti = 360 ppm, and O = 283 ppm. Since approximately 80 ppm of oxygen are required to combine with the 90 ppm of aluminum to form aluminum oxide, only 203 ppm of oxygen remained to combine with titanium, manganese, silicon, and other minor elements. Stoichiometric calculations

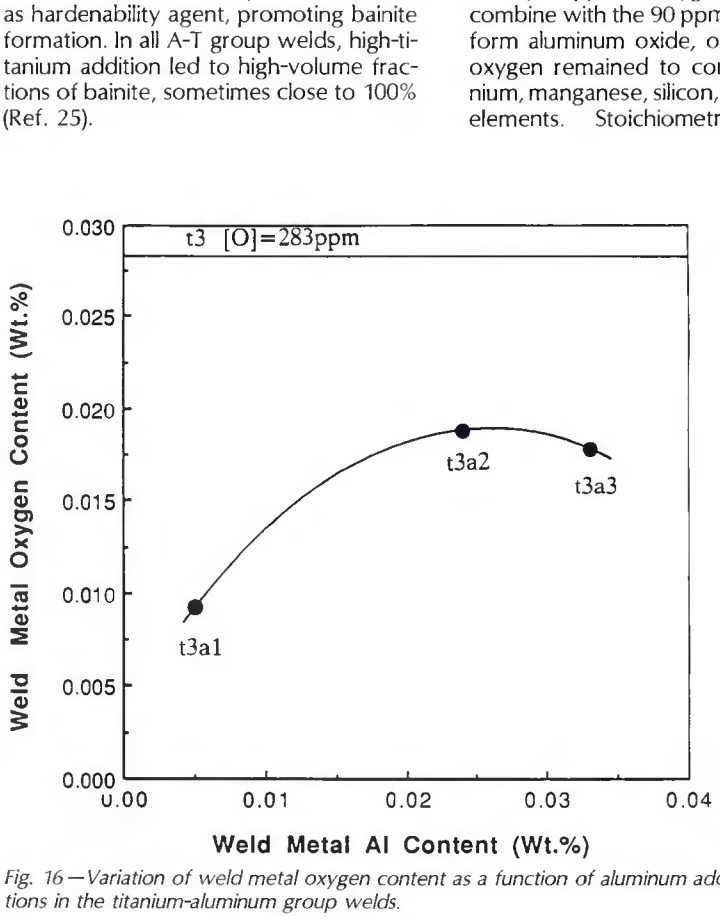

Fig. 16—Variation of weld metal oxygen content as a function of aluminum additions in the titanium-aluminum group welds.

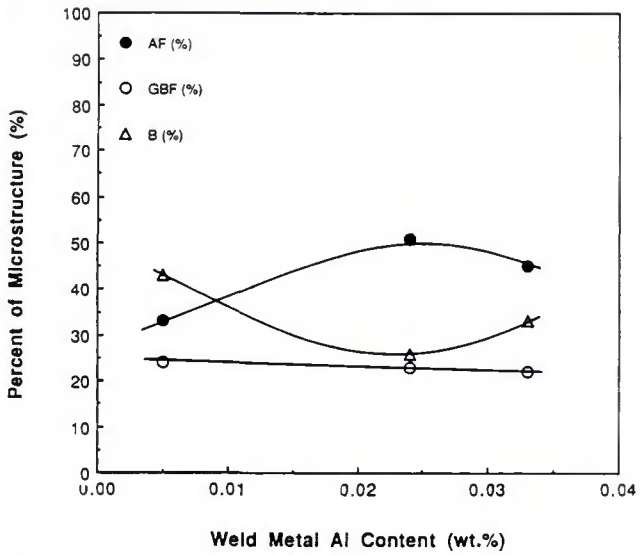

Fig. 17—Variation of weld metal microstructure as a function of aluminum additions in the titanium-aluminum group welds.

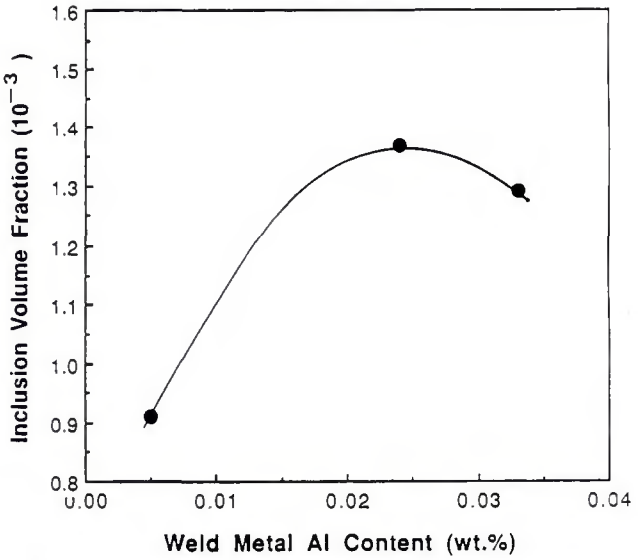

Fig. 18—Variation of inclusion volume fraction (Vv) as a function of aluminum additions in the titanium-aluminum group welds.

showed that only 120 ppm of oxygen are needed to combine with titanium to form TiO. Therefore, MnO and SiO_2 are formed and is confirmed by the inclusion analysis.

During the second pass welding, Weld t3a1, the oxygen content dropped from 283 to 93 ppm. The decrease was probably due to inclusion loss by convective flow in the weld pool, and coalescence and flotation, because Al_2O_3 inclusions are known to coalesce quite readily (Ref. 7). After adding aluminum in the second pass, Weld t3a1 contained 50 ppm of aluminum and 130 ppm of titanium. The decreasing aluminum observed was an indication that indeed inclusions were lost by flotation or convective flow in the weld pool. Assuming that all 50 ppm of aluminum are in the form of oxide, then 44 ppm of oxygen are needed. If all titanium are in the form of titanium oxide (requiring 43 ppm of oxygen), mass balance showed that only 6 ppm of oxygen would remain, which means that only very little amount of oxygen is in the form of MnO and SiO_2. This is also confirmed by inclusion analysis.

Weld t3a2 has 240 ppm of aluminum, 220 ppm of titanium, and 188 ppm of oxygen, assuming that all oxygen available has reacted with aluminum to form Al_2O_3. The 188 ppm of oxygen will combine with 212 ppm of aluminum, which means that the weld metal does not have enough oxygen to react with all aluminum. Therefore, some aluminum atoms, together with most of the titanium, manganese and silicon atoms, will remain in the weld metal as solid solution atoms and become hardenability agents. In this case, the increasing amount of titanium bearing inclusions was responsible for the increase of acicular ferrite in the weld metal.

Following the similar procedure, the 178 ppm of oxygen in Weld t3a3 were calculated to combine with 200 of the 330 ppm of aluminum to form Al_2O_3, which means that at least 130 ppm of aluminum, most of titanium (190 ppm), manganese and silicon atoms remained in the form of solid solution and promoted bainite formation.

Additionally, the optimal aluminum concentration and acicular ferrite volume fraction could also be explained as the result of an increase in inclusion volume fraction—Fig. 18. Above 0.023 wt-% of aluminum, considerable amounts of aluminum, titanium, manganese, and silicon are in solution which increased the hardenability of the alloy and promoted bainite formation at the expense of acicular ferrite. The decrease in inclusion density observed in weld specimens where aluminum concentrations were below 0.023 wt-% confirms the coalescence and floatation of aluminum oxide particles (Ref. 7).

Figure 19 illustrates the importance of deoxidation sequence by showing the microstructures of two welds with the same weld pool aluminum and titanium additions, but at different addition sequence. These micrographs show that low-carbon

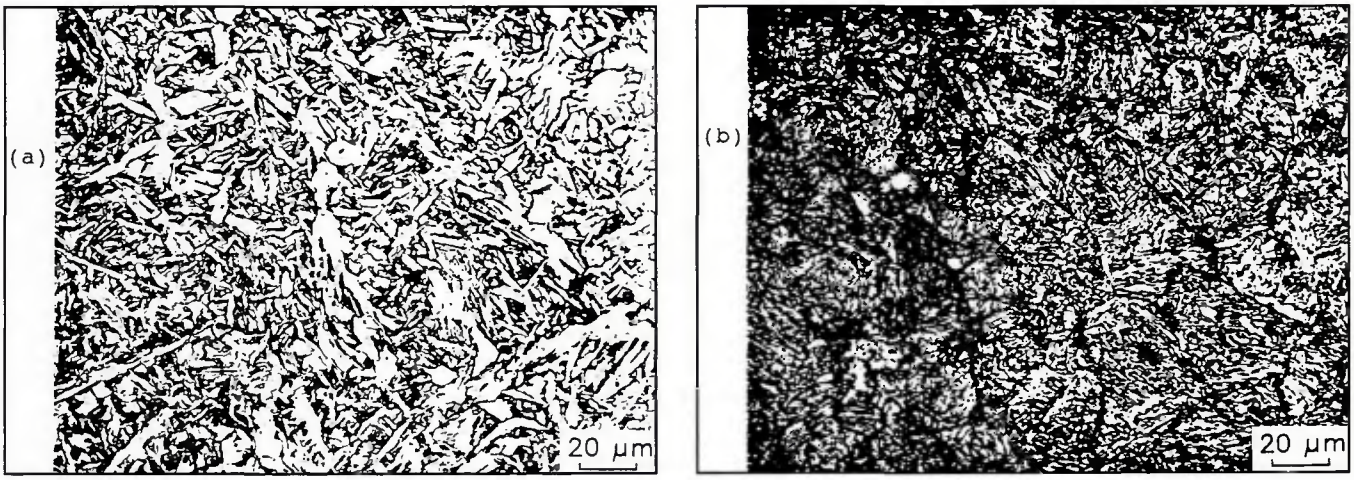

Fig. 19—Optical micrographs illustrating the importance of deoxidation sequence on weld metal microstructure. A—T1A1, predominantly grain boundary ferrite, SP and acicular ferrite; B—A1T1, predominantly bainite.

steel weld metal microstructure is indeed a function of deoxidation sequence. The titanium-aluminum sequence weld (Fig. 19A), showed a mixture of grain boundary ferrite, Widmanstätten sideplate ferrite, and acicular ferrite, while the aluminum-titanium weld (Fig. 19B) exhibited almost exclusively bainite. In the case of the latter weld, the small amount of oxygen remaining after deoxidation with aluminum was insufficient to react with titanium to form titanium oxide. The lack of nucleation sites for acicular ferrite and higher acid-soluble titanium content contributed to the bainitic microstructure.

To utilize the beneficial effects of deoxidation sequence as discussed previously, different types of electrodes must be used on multipass welding. As an example, in thick-plate fabrication using tandem welding, the chemical composition of the electrodes can be customized such that the sequence of addition of deoxidizers into the weld pool can be controlled to maximize acicular ferrite in the weld metal. From the present work, it is known that the titanium-aluminum sequence is preferred. Then, the combination of leading electrodes that contain adequate amounts of titanium followed by trailing electrodes with optimal aluminum content will result in improved microstructure and mechanical properties. The sequenced deoxidation will also result in weld metal oxygen levels much lower than those achieved by individual or simultaneous additions of deoxidizers.

Conclusions

The results of this investigation on aluminum and titanium deoxidation sequence can be summarized in the following:

Individual Effect

1) Increasing weld metal titanium content up to approximately 0.05 wt-% increased the amount of acicular ferrite and grain boundary ferrite at the expense of bainite. At titanium contents above 0.05 wt-%, both acicular ferrite and grain boundary ferrite are replaced by bainite.

2) Increasing weld metal aluminum content up to approximately 0.055 wt-% increased the amount of acicular ferrite and bainite at the expense of grain boundary ferrite. High aluminum content, that is, above 0.055 wt-%, resulted in less acicular ferrite.

3) Titanium-containing inclusions have better austenite grain boundary pinning effect than aluminum-bearing inclusions.

4) Weld metal with a larger amount of acicular ferrite are found to exhibit coarser prior austenite grains with a large number of nonmetallic inclusions of diameter around 0.45 μm.

Combined Effect

1) Deoxidation sequence is important in weld pool deoxidation and microstructural refinement. Aluminum and titanium (in solid solution) increase the weld metal hardenability which results in increasing bainite.

2) In the aluminum-titanium (A-T) group welds, higher titanium additions resulted in higher titanium in solution, which led to higher volume fraction of bainite.

3) In the titanium-aluminum (T-A) group welds, no matter how high the aluminum addition, the weld metal microstructure always show a mixture of bainite, grain boundary ferrite and acicular ferrite.

4) The concept of welding systems using multiple wires (in tandem) that contain different deoxidizers can be used to better control and refine the weld metal microstructure.

Acknowledgment

The authors appreciate and acknowledge the research support of the Office of Naval Research.

References

1. Abson, D. J. 1978. *The Role of Inclusions in controlling Weld Metal Microstructures in C-Mn Steels.* The Welding Institute, Cambridge, England.

2. Ferrante, M., and Farrar, R. A. 1982. The role of oxygen-rich inclusions in determining the microstructure of weld metal deposits. *Journal of Materials Science* 17:3293.

3. Bhadeshia, H. K. D. H., and Svensson, L.-E. 1991. Modelling the evolution of microstructure in steel weld metal. IIW DOC II-A-846-91.

4. Ricks, R. A., Howell, P. R., and Barrite, G. S. 1982. The nature of acicular ferrite in HSLA steel weld metals. *Journal of Materials Science* 17:732.

5. Liu, S., and Olson, D. L. 1986. The role of inclusions in controlling HSLA steel weld microstructures. *Welding Journal* 65(6):139-s to 150-s.

6. Choi, C. S., and Eagar, T. W. 1981. Slag-metal equilibrium during submerged arc welding. *Met. Trans. A* 12B:539-547.

7. Kluken, A. O., and Grong, O. 1989. Mechanisms of inclusion formation in Al-Ti-Si-Mn deoxidized steel weld metals. *Met. Trans. A* 20(8):1335-1349.

8. Twidwell, L. G. *Physical Chemistry of Iron and Steelmaking.* Montana College of Mineral Science and Technology.

9. USS. 1971. *The Making, Shaping and Treating of Steel.* ed., H. E. McGannon. United States Steel Corp.

10. Falconi Campos, V. 1974. Theory of deoxidation. *Deoxidation and Solidification of Steels.* Associação Brasileira de Metais.

11. Kiessling, R. 1978. *Non-metallic Inclusions in Steels. Part HV.* The Metal Society, London, England.

12. Ito, Y., and Bessyo, K. 1968. Weldability formula of high strength steels related to heat-affected zone cracking. IIW DOC IX-576-68.

13. Brownlee, J. K. 1985. Effects of aluminum and titanium on the microstructure and properties of microalloyed steel weld metal. Colorado School of Mines, M. Sc. Thesis No. T-3064, Golden, Colo.

14. Barbaro, F. J., Krauklis, P., and Easterling, K. E. 1989. Formation of acicular ferrite at oxide particles in steels. *Materials Science and Technology* 5(11):1058-1068.

15. Jang, J. W., Shah, S., and Indacochea, J. E. 1987. Influence of SAW fluxes on low-carbon steel weld microstructure. *Journal of Materials for Energy Systems* 8(4):391-401.

16. Cochrane, R. C., Ward, J. L., and Keville, B. R. 1983. The influence of deoxidation and/or desulphurisation practice on the weld metal toughness of high dilution welds. *The Effect of Residual, Impurity and Micro-alloying Elements on Weldability and Weld Properties.* Paper 16, The Welding Institute, U.K.

17. Kohno, R., Takami, T., Mori, N., and Nagano, K. 1982. New fluxes of improved weld metal toughness for HSLA steels. *Welding Journal* 61(12):373-s to 380-s.

18. Mori, N., Homma, H., Ohkita, S., and Wakabayashi, M. 1981. Mechanisms of notch toughness improvement in Ti-B-bearing weld metals. IIW DOC IX-1196-81.

19. Mori, N., Homma, H., Wakabayashi, M., and Ohkita, S. 1982. Characteristics of mechanical properties of Ti-B-bearing weld metals. IIW DOC IX-980-82.

20. Liu, S. 1984. The role of nonmetallic inclusions in controlling weld metal microstructures in niobium microalloyed steels. Colorado School of Mines, Ph.D. Thesis T-2923, Golden, Colo.

21. Liu, S., and Olson, D. L. 1987. The influence of inclusion chemical composition on weld metal microstructure. *Journal of Materials Engineering* 9(3):237-251.

22. Bhatti, A. R., Saggese, M. E., Hawkins, D. N., Whiteman, J. A., and Golding, M. S. 1984. Analysis of inclusions in submerged arc weld in microalloyed steels. *Welding Journal* 63(7): 224-s to 230-s.

23. Suzuki, S., Weatherly, G. C., and Houghton, D. C. 1987. The response of carbo-nitride particles in HSLA steels to weld thermal cycles. *Acta. Met.* 35(2):341-352.

24. Es-Souni, M., and Beaven, P. A. 1989. Microanalysis of inclusion/matrix interfaces in weld metals. *Application of Surface and Interface Analysis-ECASIA 89.* Antibes, France.

25. Liao, F. C. 1990. The effect of deoxidation sequence on carbon manganese steel weld metal microstructures. Colorado School of Mines, M. Sc. Thesis No. T-3928, Golden, Colo.